Electronic Journal of Biotechnology 60 (2022) 43–57

Contents lists available at ScienceDirect

Electronic Journal of Biotechnology

journal homepage: www.elsevier.com/locate/ejbt

Research Article

Upregulation of ITGAV and the underlying mechanisms in nasopharyngeal carcinoma ☆

Si-Wei Huang [a], Jia-Yuan Luo [a], Li-Ting Qin [a], Su-Ning Huang [b], Zhi-Guang Huang [a], Yi-Wu Dang [a], Juan He [a], Jiang-Hui Zeng [c], Zhu-Xin Wei [d], Wei Lu [e], Gang Chen [a,*]

[a] Department of Pathology, The First Affiliated Hospital of Guangxi Medical University, No.6 Shuangyong Road, Nanning, Guangxi Zhuang Autonomous Region 530031, PR China
[b] Department of Radiotherapy, Guangxi Medical University Cancer Hospital, No.71 Hedi Rd, Nanning, Guangxi Zhuang Autonomous Region 530021, PR China
[c] Department of Clinical Laboratory, The Third Affiliated Hospital of Guangxi Medical University/Nanning Second People's Hospital, No. 13 Dancun Road, Nanning, Guangxi Zhuang Autonomous Region 530031, PR China
[d] Department of Radiotherapy, The First Affiliated Hospital of Guangxi Medical University, No.6 Shuangyong Road, Nanning, Guangxi Zhuang Autonomous Region 530031, PR China
[e] Department of Pathology, The Third Affiliated Hospital of Guangxi Medical University/Nanning Second People's Hospital, No. 13 Dancun Road, Nanning, Guangxi Zhuang Autonomous Region 530031, PR China

GRAPHICAL ABSTRACT

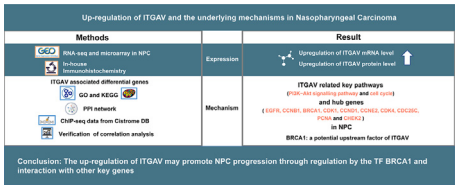

ARTICLE INFO

Article history:
Received 10 January 2022
Accepted 6 September 2022
Available online 13 September 2022

Keywords:
BRCA1
Breast cancer
Cancer
Cell cycle
Gene chip
Integrin
ITGAV
Nasopharyngeal carcinoma
immunohistochemistry

ABSTRACT

Background: Integrin subunit α -v (ITGAV) has been demonstrated to be dysregulated and involved in cancer promotion processes in a variety of cancers, but studies on nasopharyngeal carcinoma (NPC) have been limited. Our study aimed to comprehensively assess the expression level and potential mechanisms of ITGAV in NPC.

Results: A total of 13 mRNA expression datasets and internal tissue microarrays were included. ITGAV protein and mRNA were overexpressed in NPC. The pathways of upregulated genes positively related to ITGAV in NPC were analyzed, and the PI3K–Akt signaling pathway, cell cycle, and human papillomavirus infections were most significantly enriched. The protein–protein interaction network was constructed for the genes enriched in these pathways, and the corresponding hub genes were obtained. Among them, breast cancer susceptibility gene 1 (BRCA1) was predicted to be a transcription factor of ITGAV via the Cistrome DB Toolkit, which was also confirmed by ChIP-seq information and correlation calculations.

Conclusions: ITGAV is overexpressed in NPC and can regulate BRCA1 to participate in the cancer process. ITGAV serves as a potential therapeutic target in NPC patients.

Abbreviations: AUC, Area under the curve; BRCA1, Breast cancer susceptibility gene 1; CI, Confidence interval; DEGs, Differentially expressed genes; ECM, Extracellular matrix; GEO, Gene Expression Omnibus; GO, Gene Ontology; IHC, Immunohistochemical; IRS, Immunoreactivity score; ITGAV, Integrin subunit α-V; I^2, I-square; KEGG, Kyoto Encyclopedia of Genes and Genomes; NPC, Nasopharyngeal carcinoma; NCBI, National Center for Biotechnology Information; PPI, Protein-protein interaction; ROC, Receiver operating characteristic; SMD, Standard mean deviation; SROC, Summary receiver operating characteristic; TCGA, The Cancer Genome Atlas; TFs, Transcription factors.

Peer review under responsibility of Pontificia Universidad Católica de Valparaíso

* Corresponding author.
E-mail address: chengang@gxmu.edu.cn (G. Chen).

https://doi.org/10.1016/j.ejbt.2022.09.002

Therapeutic target
Transcription factors

How to cite: Huang S-W, Luo J-Y, Qin L-T, et al. Upregulation of ITGAV and the underlying mechanisms in nasopharyngeal carcinoma. Electron J Biotechnol 2022;60. https://doi.org/10.1016/j.ejbt.2022.09.002.

1. Introduction

Nasopharyngeal carcinoma (NPC) is a special malignant tumor originating from the nasopharyngeal epithelial lining; it has a high incidence in southern China, North Africa, and Southeast Asia. Recently, the epidemiological trend of NPC has been studied, and the results indicate that the incidence rate and death rate are gradually decreasing. In addition, plasma Epstein-Barr virus DNA has been used for population screening [1,2,3,4,5,6,7]. Although significant progress has been made in the screening and treatment of NPC, the five-year survival rate of patients with advanced NPC has not obviously improved [8,9,10,11]. Therefore, it is necessary to probe the potential pathogenesis of NPC and find possible therapeutic targets.

As the main cell adhesion receptor of the extracellular matrix (ECM) component, integrin is a family of 24 transmembrane heterodimers produced by the combination of 18α integrin and 8β integrin subunits, and changes in this structure have often been detected in cancer [12]. New blood vessels formed from the preexisting ones can enhance tumor growth, and these blood vessels can act as channels of tumor cell metastasis. As a family of cell surface ECM receptors, integrins can facilitate endothelial cell migration and survival [13]. α5β1, α5β3, and α5β5 integrins, which regulate angiogenesis in different ways all contain the integrin subunit α-V (ITGAV) [14]. ITGAV disorder is closely associated with the occurrence and development of various cancers, including gastric cancer, hepatocellular carcinoma, breast cancer, and osteosarcoma [15,16,17,18]. However, only a few research studies have focused on the relationship between ITGAV and NPC. Shi et al. collected clinical samples and detected the expression of ITGAV in NPC tissues using the real-time polymerase chain reaction method and immunohistochemistry (IHC) staining method; the results showed that ITGAV overexpression is closely related to the metastasis and progression of NPC [19]. Ou et al. confirmed that ITGAV induces multicellular radio-resistance in human NPC by activating the SAPK/JNK pathway [20]. In addition, ITGAV has been found to be involved in the epithelial-mesenchymal transition of NPC as a target gene of mir-9-3p [21]. These independent studies have provided different valuable views on the role of ITGAV in NPC, but because of the small number of studies, the ability to discover the complex molecular mechanisms of NPC is still limited.

In this study, pathological samples diagnosed as NPC and normal nasopharyngeal tissues were collected at the First Affiliated Hospital of Guangxi Medical University to further verify the expression pattern of ITGAV on a protein level. Then, all available datasets were gathered from Gene Expression Omnibus (GEO), ArrayExpress, Oncomine, the Cancer Genome Atlas (TCGA) and the literature, which were applied to analyze the expression pattern and clinical pathology significance of ITGAV in NPC. Subsequently, we systematically integrated all the information of ITGAV and predicted its upstream transcription factors (TFs) to explore the potential mechanism of ITGAV and new biomarkers in NPC. A flowchart of this research and the retrieval strategy are shown in Fig. 1.

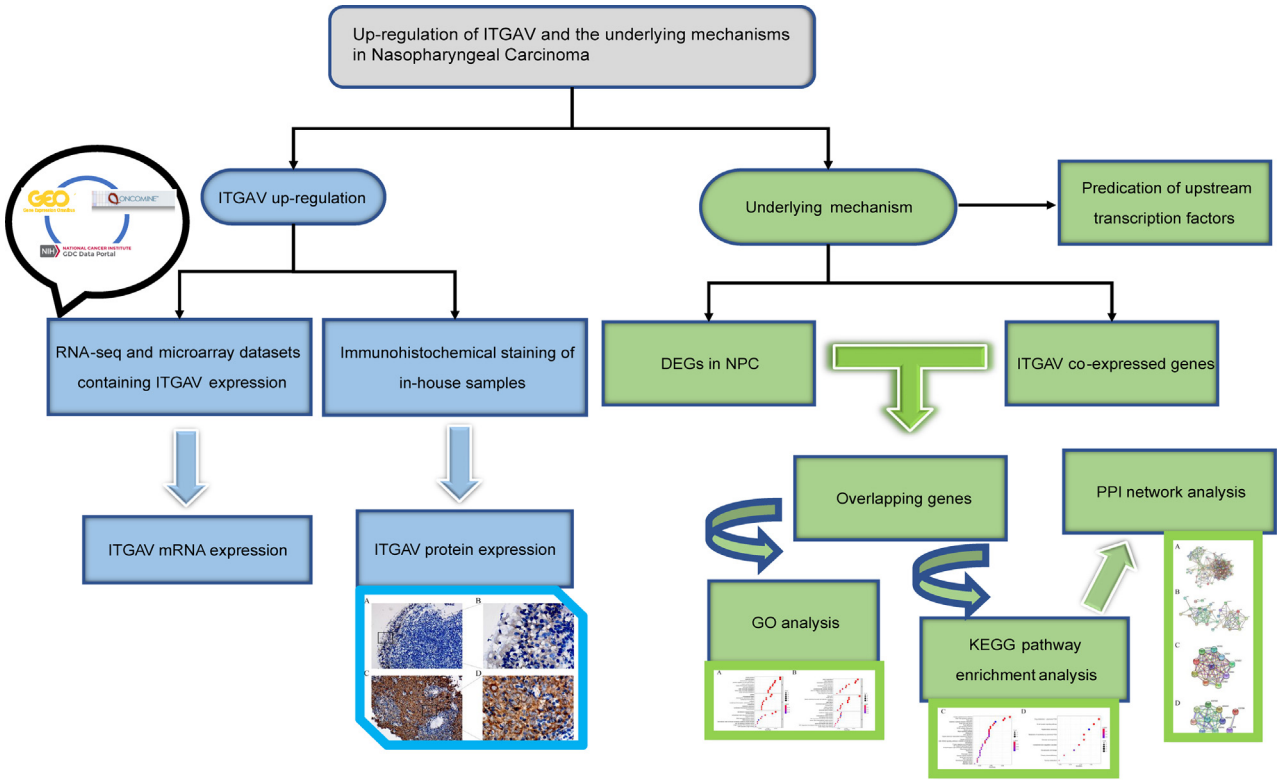

Fig. 1. Flow chart of the study.

2. Materials and Methods

2.1. Inhouse immunohistochemical staining and evaluation

In this study, 98 clinical specimens were subjected to immunohistochemical (IHC) staining to detect the protein expression level of ITGAV. The 98 samples included 67 NPC cases and 31 control nasopharyngeal cases. All participating patients signed informed consent forms, and the study was approved by the ethics committee of the First Affiliated Hospital of Guangxi Medical University. All IHC processes were performed in accordance with the protocol of the manufacturer. The regional differences in staining were assessed by immunoreactivity score (IRS). Under an optical microscope, 10 typical, high-power fields were randomly observed. The final IRS consists of two parameters: the intensity of staining and the percentage of stained cells in each sample. The staining intensity values 0, 1, 2, and 3 represented the staining status of a sample as unstained, weakly stained, moderately stained, and strongly stained, respectively. Percentage of stained cells was also recorded. If no cells were stained, the percentage of stained cells was recorded as 0; if <10% of cells were stained, the percentage of stained cells was recorded as 1; if 11–50% of the cells were stained, the percentage of stained cells was recorded as 2; if 51–80% of the cells were stained, the percentage of stained cells was recorded as 3; if the percentage of stained cells exceeded 80%, the percentage of stained cells was recorded as 4. The above two scores were multiplied to generate an IRS in the range of 0–12 [22,23,24]. The IRS of each group was performed with independent sample t-test using IBM SPSS Statistics 23.0 statistical software.

2.2. Data search and screening

The search formula (nasopharyngeal OR nasopharynx) AND (neoplasm OR cancer OR tumor OR carcinoma OR malignancy) was used to search on GEO (https://www.ncbi.nlm.nih.gov/geo/) so that the microarray or RNA-seq data set for the evaluation of ITGAV expression patterns and related clinical information could be found. The conditions for data selection were as follows: (i) The data set must contain the expression profile data of ITGAV in NPC that can be used for analysis; (ii) The data set must contain at least three normal nasopharyngeal samples and three NPC samples; (iii) Each sample must be an original sample obtained from an untreated patient or cell line. The search method was also used on the TCGA data portal (https://cancergenome.nih.gov/) and Oncomine (https://www.oncomine.org/resource/main.html). To avoid missing additional related research, we examined Chinese and English databases, such as PubMed, MEDLINE, Embase, Cochrane Library, Web of Science, CNKI, and Wanfang. The retrieved characters were as follows: (ITGAV OR Integrin alpha V OR CD51) AND (nasopharyngeal OR nasopharynx) AND (neoplasm OR cancer OR tumor OR carcinoma OR malignancy). The relevant research filtering strategies are shown in Fig. 2. The last retrieval date was February 1, 2021.

2.3. Comprehensive analysis of the expression level of ITGAV mRNA in NPC

After normalizing the collected data, we extracted the expression data of ITGAV from all processed datasets for subsequent analysis, and different datasets from the same sequencing platform

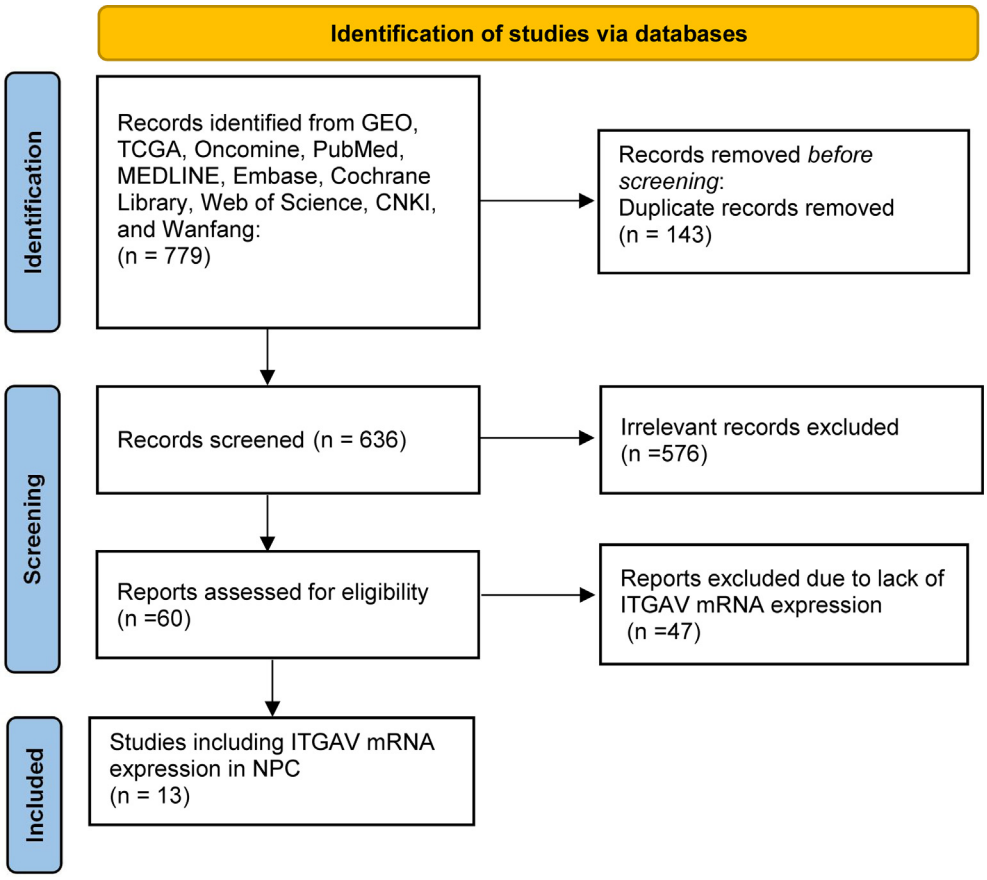

Fig. 2. Retrieval strategy schematic.

were integrated. The violin graph and receiver operating characteristic (ROC) graph of each data set were drawn by GraphPad Prism 8.0 to visually display the expression pattern of ITGAV mRNA in each data set. The standard mean deviation (SMD) and the 95% confidence interval (CI) of the SMD were calculated by IBM SPSS Statistics 23.0 and STATA 16.0 software. SMD>0 indicated that the expression level of ITGAV in cancerous tissues was higher than that in noncancerous tissues. If the 95% CI did not contain 0, it was considered statistically significant. The I-square (I^2) test was used to analyze the heterogeneity of each study. I^2>50% or p value<0.05 demonstrated that the study was heterogeneous. A fixed-effects model or a random effects model was chosen as decided by the analysis of heterogeneity. To further determine the ability of ITGAV to distinguish between NPC and noncancerous nasopharyngeal tissue, a summary receiver operating characteristic (SROC) curve was generated based on sensitivity and specificity, and the area under the curve (AUC) was obtained. A Fagan inspection was also performed. To ensure the stability of the results, the Begg funnel chart and Egger test were used to test publication bias. A p value of >0.05 was considered no significant publication bias [25,26,27].

2.4. Screening strategy of differential genes in NPC and ITGAV co-expressed genes

The Bioconductor Limma software package was used in R 4.0.2 software, and the filter condition was set to (i) | log FoldChange | > 1. The adjusted p value was <0.05. To obtain more accurate differentially expressed genes (DEGs), we calculated the SMD of the

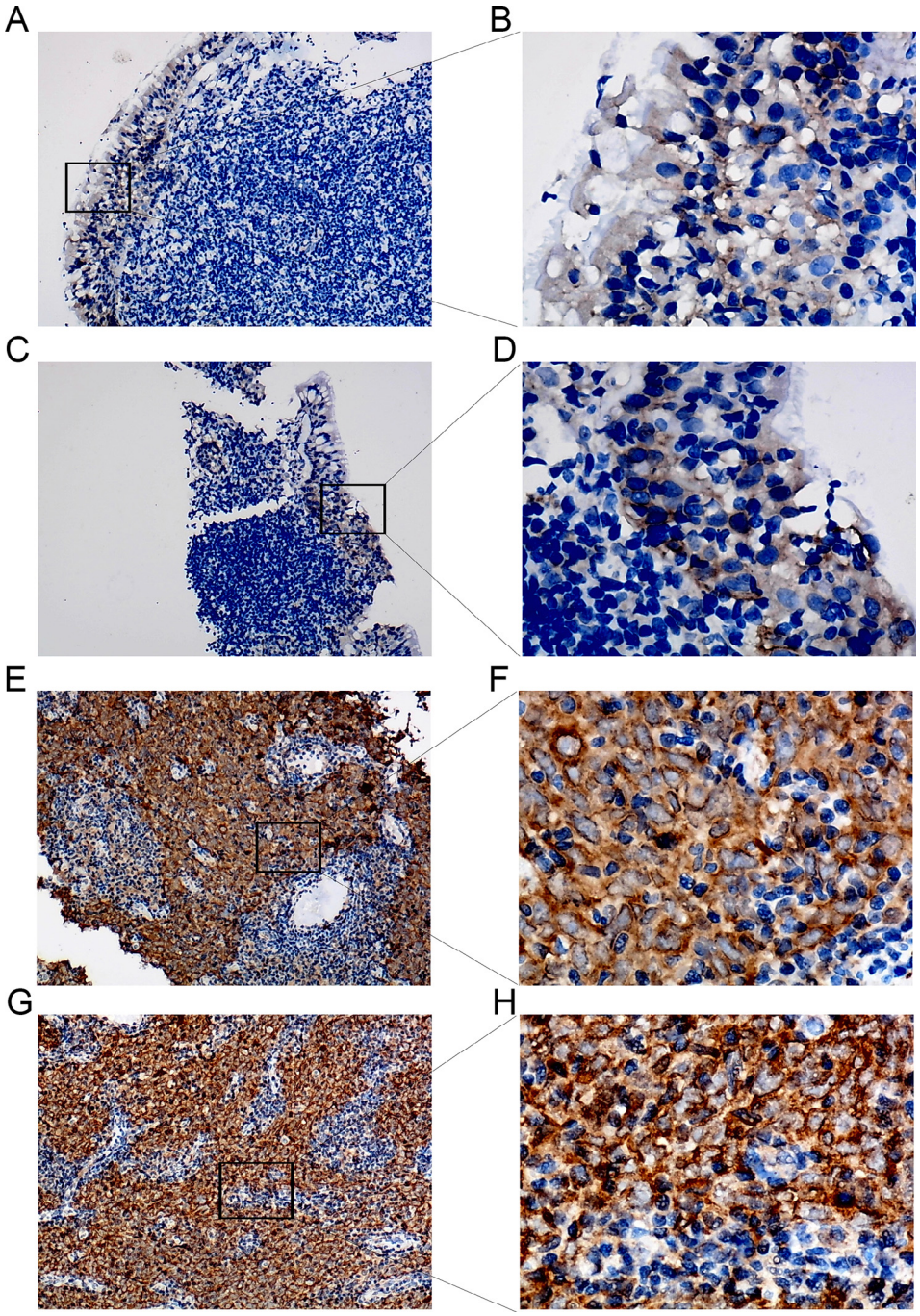

Fig. 3. ITGAV protein expression in nasopharyngeal carcinoma and normal tissues assessed by IHC. (A ∼ D) A normal nasopharyngeal tissue shows low ITGAV expression. (E ∼ H) A nasopharyngeal carcinoma tissue shows high ITGAV expression. Magnification: ×100 (A, C, E, G) and × 400 (B, D, F, H).

Table 1
Characteristics of microarray datasets included in the study. Note: Mean1 ± SD1: nasopharyngeal carcinoma tissues; Mean0 ± SD0: nontumor tissues. SD: standard deviation.

Study	Country	Cancer group	Normal control	Mean1 ± SD1	Mean0 ± SD0
GPL570(GSE64634, GSE34573, GSE12452)	China, UK, USA	58	17	11.47 ± 0.79	9.96 ± 1.34
GPL11154(GSE68799, GSE63381, GSE102349)	China, Singapore, USA	159	4	4.56 ± 0.76	2.30 ± 0.33
GPL96 (GSE13597)	UK	25	3	8.78 ± 0.73	6.84 ± 1.06
GPL6244 (GSE39826)	UK	3	3	8.89 ± 0.02	10.37 ± 0.05
GPL8380(GSE40290)	China	25	8	−0.03 ± 0.92	−1.60 ± 0.56
GPL6480 (GSE53819)	China	18	18	11.79 ± 0.72	10.48 ± 0.44
GPL19061 (GSE61218)	China	10	6	8.37 ± 0.80	6.88 ± 0.75
GPL20301 (GSE118719)	USA	7	4	8.20 ± 0.71	6.27 ± 0.47
GPL16956 (GSE126683)	China	3	3	7.54 ± 0.14	7.16 ± 0.08
In-house IHC	China	67	31	9.29 ± 1.91	1.97 ± 1.45

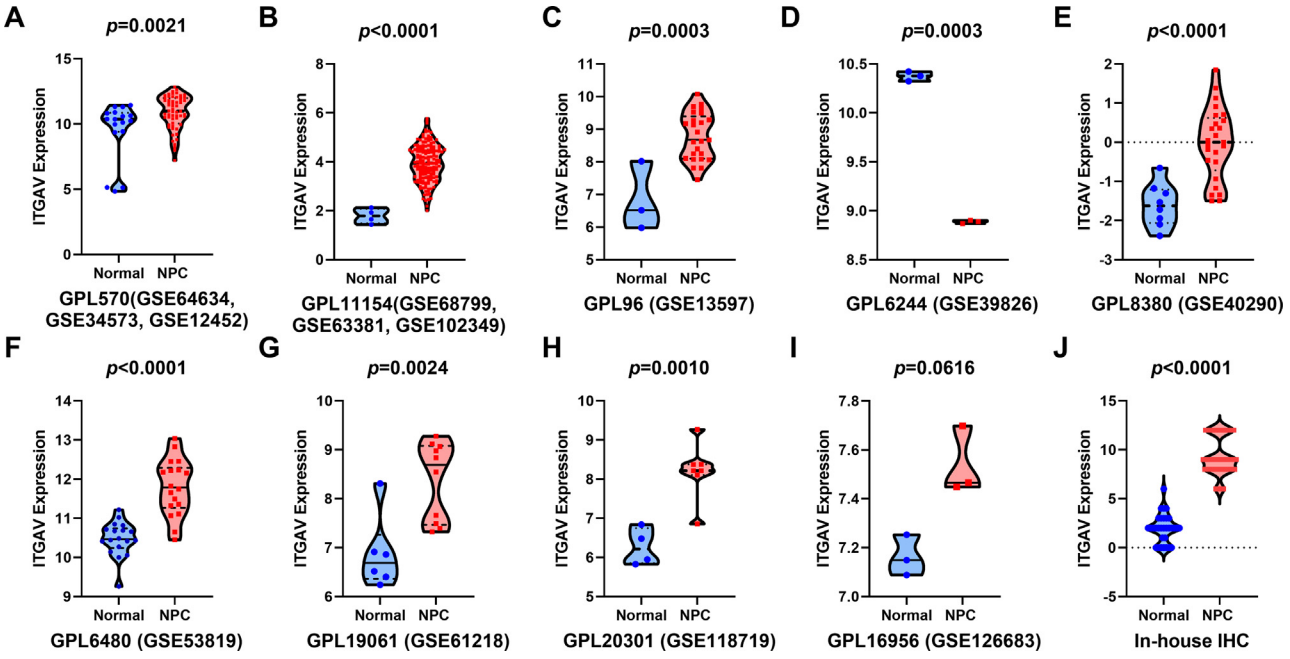

Fig. 4. (A)-(J) Different expression levels of ITGAV between nasopharyngeal carcinoma and normal nasopharynx tissues based on nine datasets and in-house IHC.

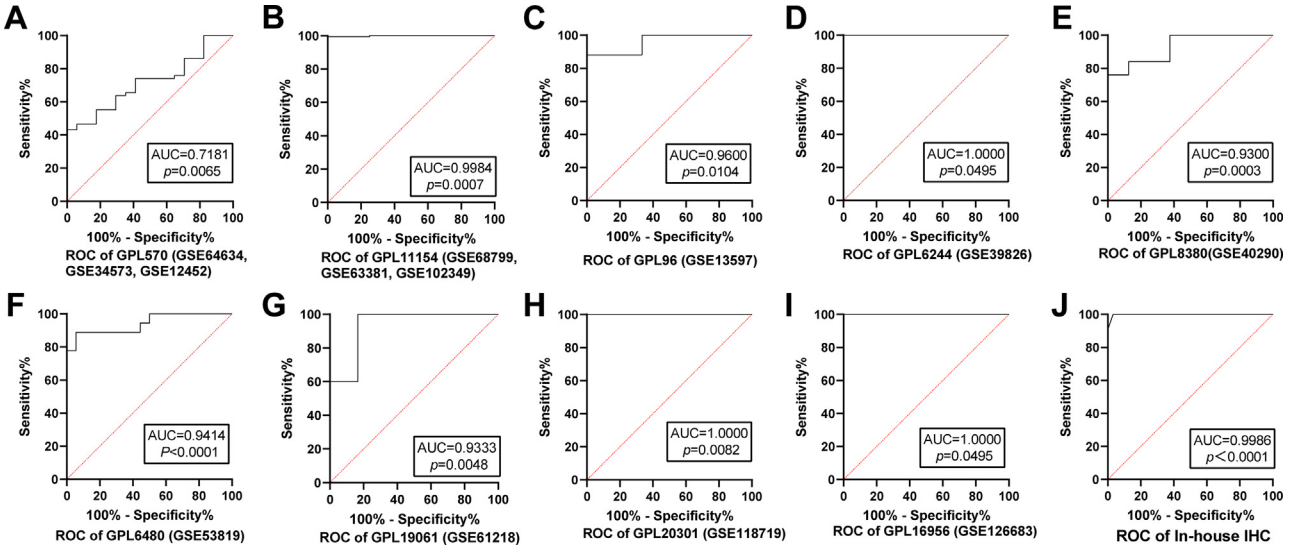

Fig. 5. (A)-(I) ROC curves of ITGAV mRNA and protein. (J) Expression between nasopharynx cancer and nontumour tissues.

above genes. These genes that 95% CI of SMD did not include 0 were further selected. The Pearson correlation algorithm was used to screen the co-expressed genes of ITGAV, and the screening conditions were as follows: (i) |correlation coefficient| $\geq$ 0.3 and (ii) adjusted p value <0.05. According to the positive and negative signs of the r value, the co-expressed genes were divided into two groups, which were positively correlated or negatively correlated with ITGAV expression. The nine gene sets were screened separately to obtain their respective upregulated differential genes, downregulated differential genes, positively correlated co-expressed genes, and negatively correlated co-expressed genes. After aggregation, we obtained upregulated and downregulated DEGs and positively correlated and negatively correlated genes with repeat number $\geq$5 in 9 datasets. Gene intersection Ⅰ was composed of upregulated DEGs and positively related genes. The downregulated DEGs and the negatively related gene crossed to obtain gene intersection Ⅱ.

2.5. Exploration of the potential molecular mechanism of ITGAV in NPC

The clusterProfiler software package was selected to be used in R 4.0.2 software. Gene intersections Ⅰ and Ⅱ were functionally annotated by Gene Ontology (GO). Kyoto Encyclopedia of Genes and Genomes (KEGG) pathway enrichment was also carried out in R 4.0.2. The enrichment results were presented with a visual enrichment chart. STRING (https://string-db.org) was often used to analyze the interaction between proteins. The genes enriched in the first three KEGG pathways were used to construct the protein–protein interaction (PPI) network, and the corresponding TSV file was obtained. The Cytoshubba module in the Cytoscape 3.8.1 software was used to analyze the two TSV files, and the 10 hub genes with stronger protein interactions were screened. The hub genes were visualized using STRING [28,29,30].

2.6. The prediction of the upstream transcription factor of ITGAV

Cistrome DB Toolkit (http://dbtoolkit.cistrome.org/) was utilized to obtain ITGAV TFs [31]. This tool could predict a series of upstream TFs of the input gene. The regulatory potential score reflects the possibility of TF regulating target genes, which is derived from the BETA algorithm of Cistrome DB [32]. To more intuitively evaluate the potential of ITGAV combined with TF, we used the analyzed samples in the Cistrome Data Browser (https://cistrome.org/db/#/); they were visualized using the Integrative Genomics Viewer. In addition, we extracted breast cancer susceptibility gene 1 (BRCA1) expression levels from nine expression matrices and calculated SMD and SROC curves to evaluate the expression patterns. GraphPad Prism 8.0 was applied to calculate the correlation coefficient r value between ITGAV and BRCA1. Subsequently, we also obtained the base sequence near the ITGAV transcription start site from the National Center for Biotechnology Information (NCBI, https://www.ncbi.nlm.nih.gov/). Combined r values were calculated to comprehensively assess the co-expression extent of ITGAV and BRCA1. Standard error and r value cannot be used directly to calculate SMD; hence, r value was converted to Fisher's Z. Standard error was then computed, and the final result was converted back to r value.

3. Results

3.1. The verification of ITGAV expression in NPC based on independent datasets from various sources

The protein expression of ITGAV in 98 clinical samples was detected by IHC staining. According to the IRS, the protein expression of ITGAV in NPC samples (9.2836 ± 1.9054) was significantly higher than that in the control groups (1.9677 ± 1.4488, p < 0.0001, Fig. 3). Several online databases were excavated to search for an independent cohort containing the original sample of NPC mRNA expression data. The sample information for the TCGA Head and Neck squamous cell carcinoma project was checked, and no tissue originating from the nasopharynx was found, so TCGA data were not included in this study. Finally, 13 gene chips were obtained. Among them, GSE68799, GSE63381, and GSE102349 were from the same sequencing platform, GPL11154. GSE64634, GSE34573, and GSE12452 were from GPL570 (Table 1). Based on each independent data set, the expres-

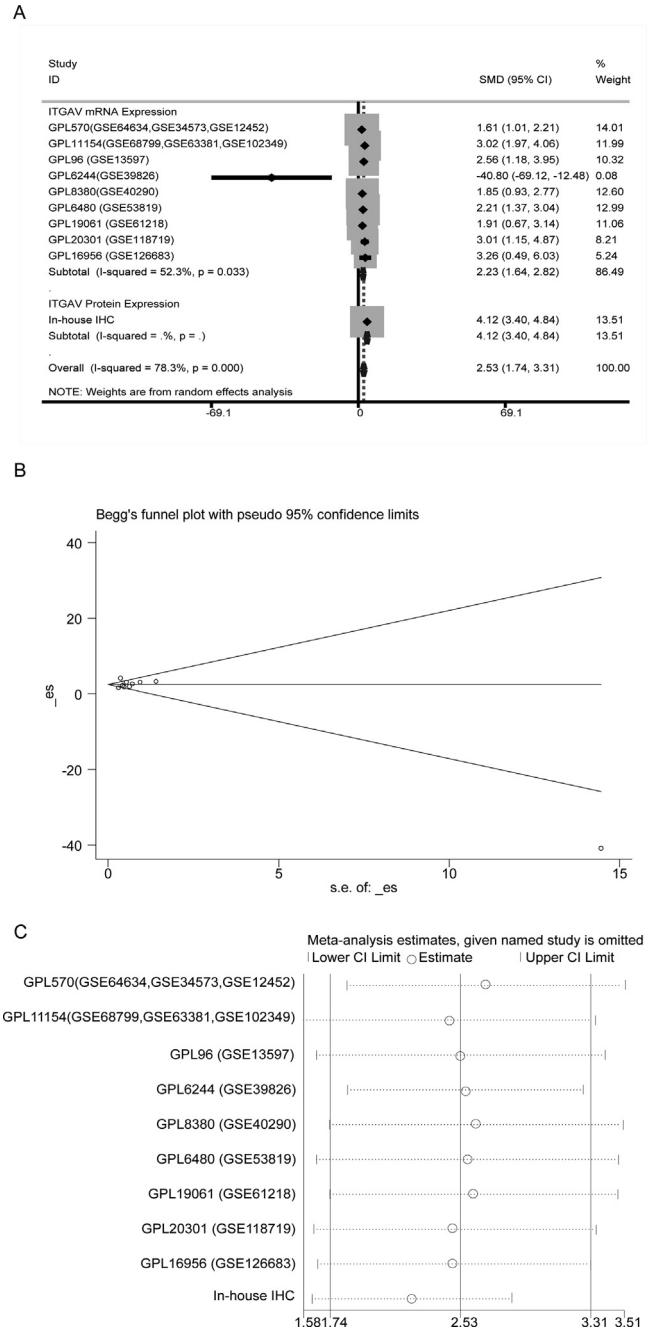

Fig. 6. The forest blot, sensitivity analysis, and Begg's funnel plot of ITGAV mRNA and protein expression. (A) Forest plot for detecting ITGAV mRNA and protein expression between nasopharynx cancer and nontumour tissues. (B) Funnel plots determine the existence of publication bias. (C) Sensitivity analysis of SMD (random effects model).

sion of ITGAV mRNA in NPC tissue and normal nasopharyngeal tissue were extracted; hence, the expression pattern of ITGAV in NPC was studied. The results were visualized by violin charts (Fig. 4) and ROC curves (Fig. 5) for each data set. It was found that the ITGAV mRNA expression level in NPC was significantly upregulated (p < 0.05; except GSE126683, p = 0.0616, and GSE39826, p = 0.0003). Among the nine gene matrices, the AUC of ROC curve of eight except GPL570 was greater than 0.8 ($p < 0.05$).

3.2. Multisample integrated analysis verifies the upregulation of ITGAV in NPC

Because of the insufficient research scale of independent datasets, it was not possible to draw effective conclusions. All the data were integrated to comprehensively analyze and verify the overexpression of ITGAV in NPC cancer tissues. The total SMD of ITGAV mRNA and protein levels were 2.53 (95% CI:1.74–3.31; Fig. 6A).

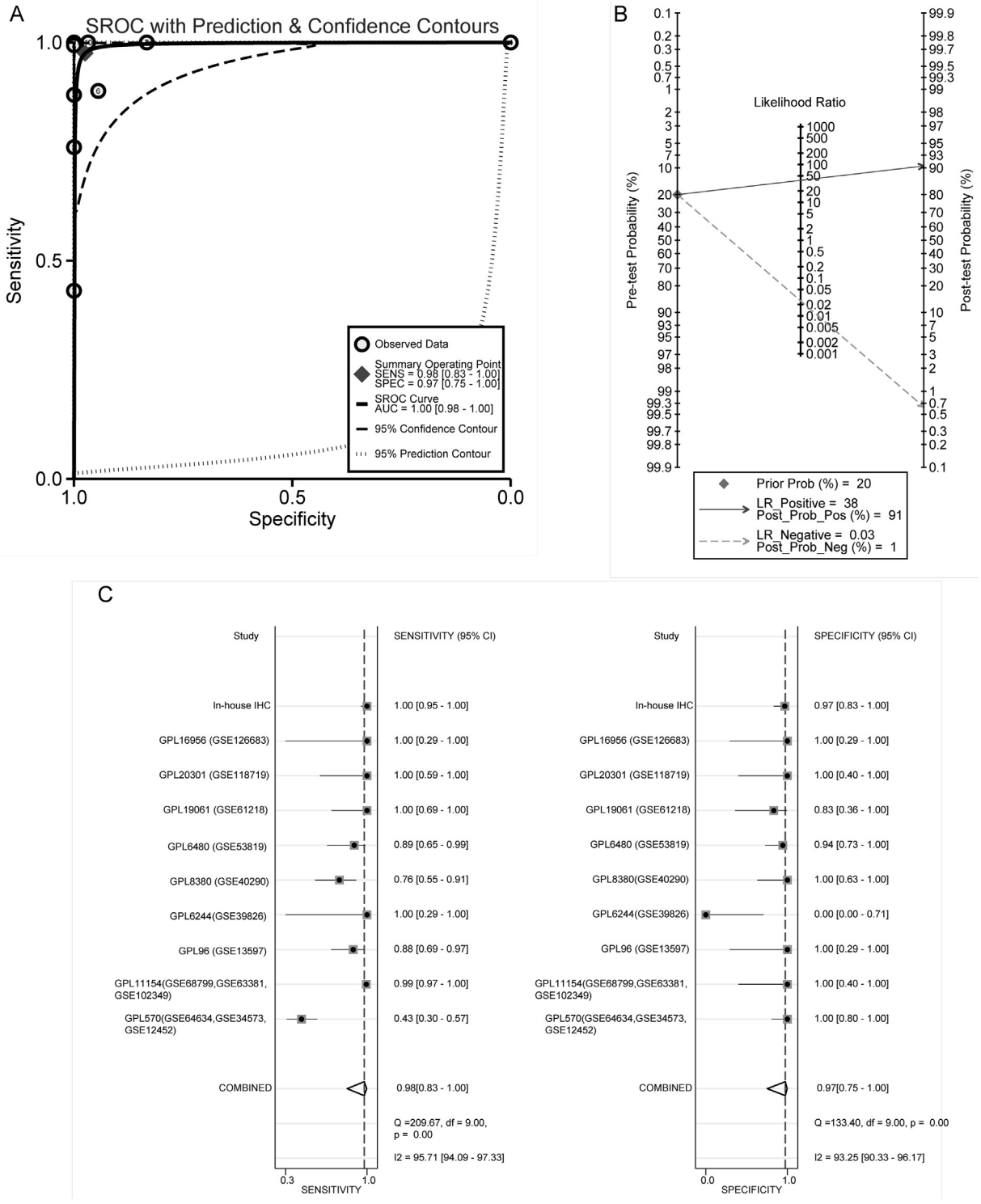

Fig. 7. Analysis of the value of ITGAV in the diagnosis of nasopharyngeal carcinoma. (A) SROC curve of the distinguishing capability of ITGAV for cancer from normal tissues; (B) Diagnostic sensitivity and specificity analysis; (C) Fagan's nomogram.

The random effects model was adopted due to the obvious heterogeneity of the results. In subgroup analysis, the SMD of ITGAV mRNA was 2.23 (95% CI: 1.64–2.82, $p < 0.001$), suggesting that ITGAV mRNA was significantly upregulated in NPC tissues. The SMD of internal clinical samples was 4.12 (95% CI: 3.40–4.84, $p < 0.001$), which also suggests that compared with normal nasopharyngeal tissue, the expression of ITGAV protein in NPC tissue was upregulated as well. Begg's funnel plot and Egger's test were also performed to visualize publication bias. No significant publication bias was found in Begg's regression chart ($p \approx 1.000$;

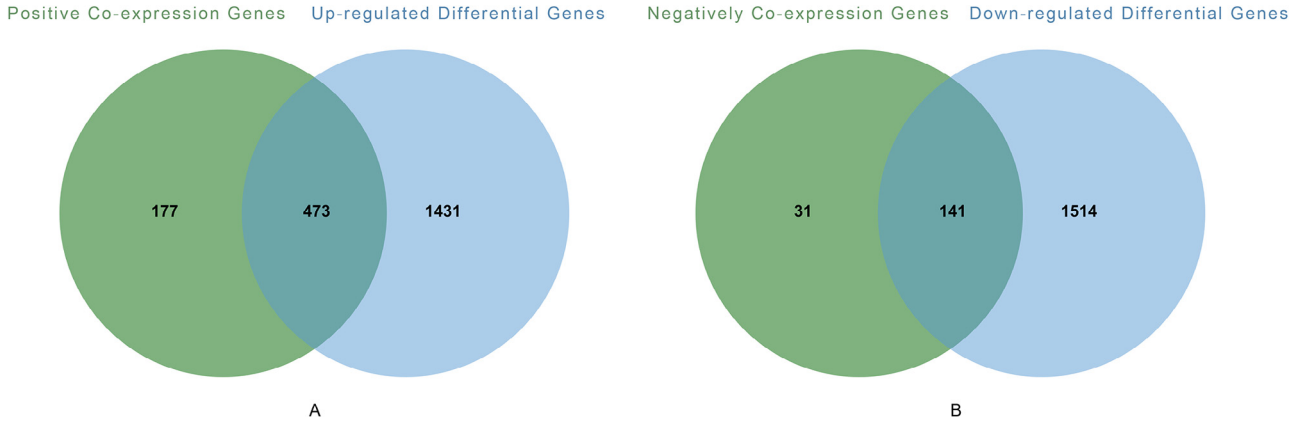

Fig. 8. Venn diagram of the intersection of ITGAV differential genes and co-expressed genes (A) Venn diagram of gene intersection Ⅰ. (B) Venn diagram of gene intersection Ⅱ.

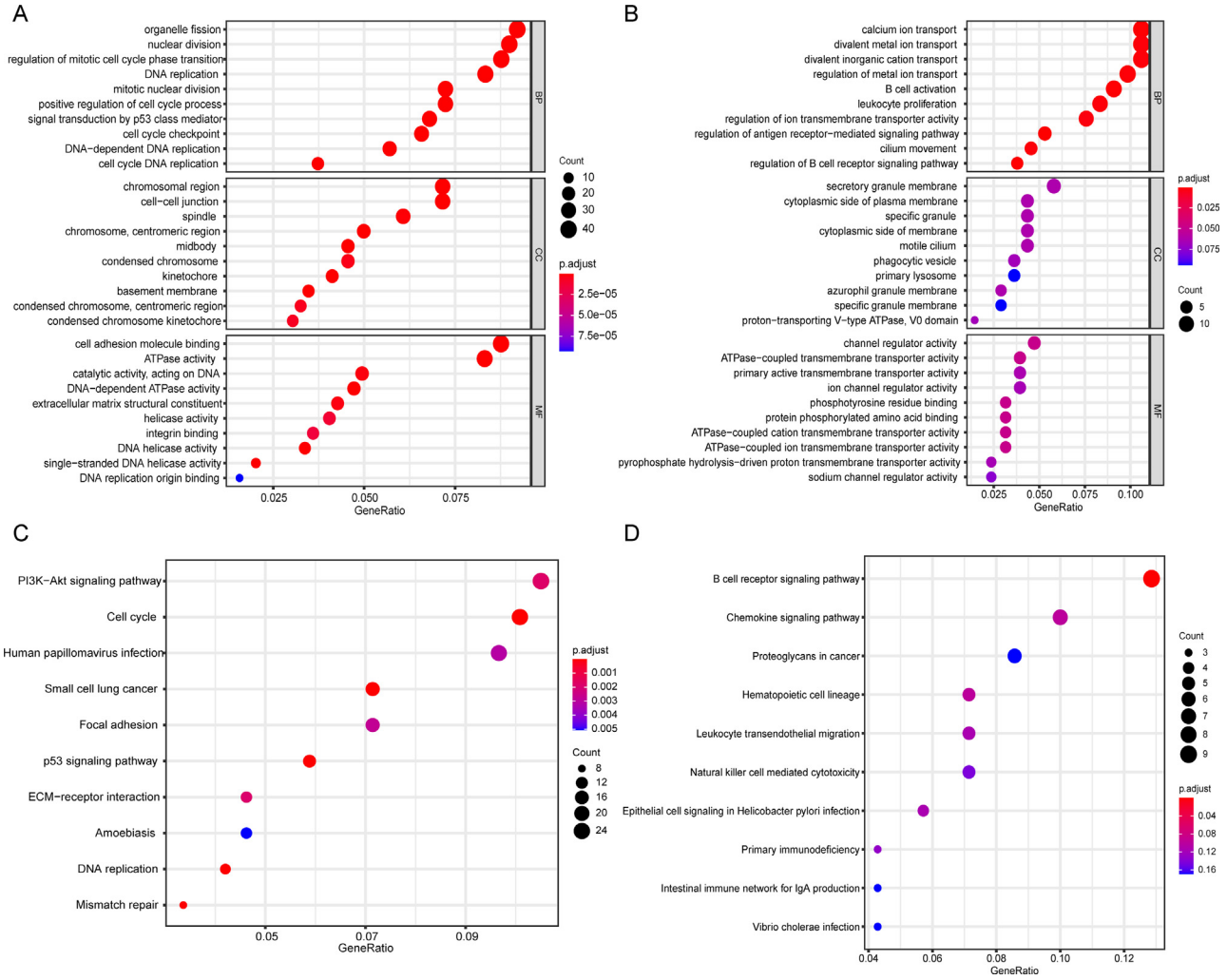

Fig. 9. Bioinformatics analysis of the potential mechanism of ITGAV in nasopharyngeal carcinoma. (A) GO of gene intersection Ⅰ. (B) GO of gene intersection Ⅱ. (C) KEGG of gene intersection Ⅰ. (D) KEGG of gene intersection Ⅱ.

Fig. 6B) and Egger's test (p = 0.567). Sensitivity analysis showed that the combined SMD was stable (Fig. 6C). To further verify that ITGAV can distinguish NPC cancer tissues from normal nasopharyngeal tissues, a SROC curve was drawn, and the AUC was calculated to be 1.00 (95% CI: 0.98–1.00; Fig. 7A). The combined sensitivity and specificity were 0.98 (95% CI: 0.83–1.00) and 0.97 (95% CI: 0.75–1.00), respectively (Fig. 7B). The Fagan diagram also confirmed the diagnostic accuracy of ITGAV for NPC (Fig. 7C).

3.3. Identification of the DEGs in NPC tissues and ITGAV co-expressed genes

After screening and integrating 13 datasets, 3,559 DEGs were collected, including 1,904 upregulated genes and 1,655 downregulated genes in NPC tissue. In addition, the 13 datasets were screened for co-expressed genes. Finally, 822 genes were co-expressed with ITGAV in NPC tissues with five or more repetitions, of which 650 were positively correlated with ITGAV expression and 172 were negatively correlated. Upregulated and positively related genes were intersected to obtain gene intersection Ⅰ, and downregulated and negatively related genes were intersected to obtain gene intersection Ⅱ (Fig. 8).

3.4. GO and KEGG enrichment analyzes

To explore the potential mechanism of ITGAV in NPC, gene intersections Ⅰ and Ⅱ containing ITGAV were analyzed for GO function enrichment. Figs. 9A and B exhibit the top ten functional items in the three types of items: biological process, cell component, and molecular function, respectively. In addition, KEGG enrichment analysis of gene intersection Ⅰ showed that the genes were related to PI3K−Akt signaling pathway, cell cycle, and human papillomavirus infection, and gene intersection Ⅱ was mainly enriched in B cell receptor signaling pathway, chemokine signaling pathway, and proteoglycans in cancer (Figs. 9C and D).

3.5. Construction of PPI network and identification of pivot genes

To understand the correlation between genes enriched in the first three pathways of KEGG, we used STRING to construct a PPI network with these enriched genes (Figs. 10A and B). The restriction conditions were set with an interaction score greater than 0.4 and a p value less than 0.05. The CytoHubba module in the Cytoscape 3.8.1 software used an indexing algorithm to screen the top hub genes in gene intersections Ⅰ and Ⅱ. For gene intersection Ⅰ, the hub genes were EGFR, CCNB1, BRCA1, CDK1, CCND1, CCNE2, CDK4, CDC25C, PCNA, and CHEK2 (scores: 27, 26, 26, 25,

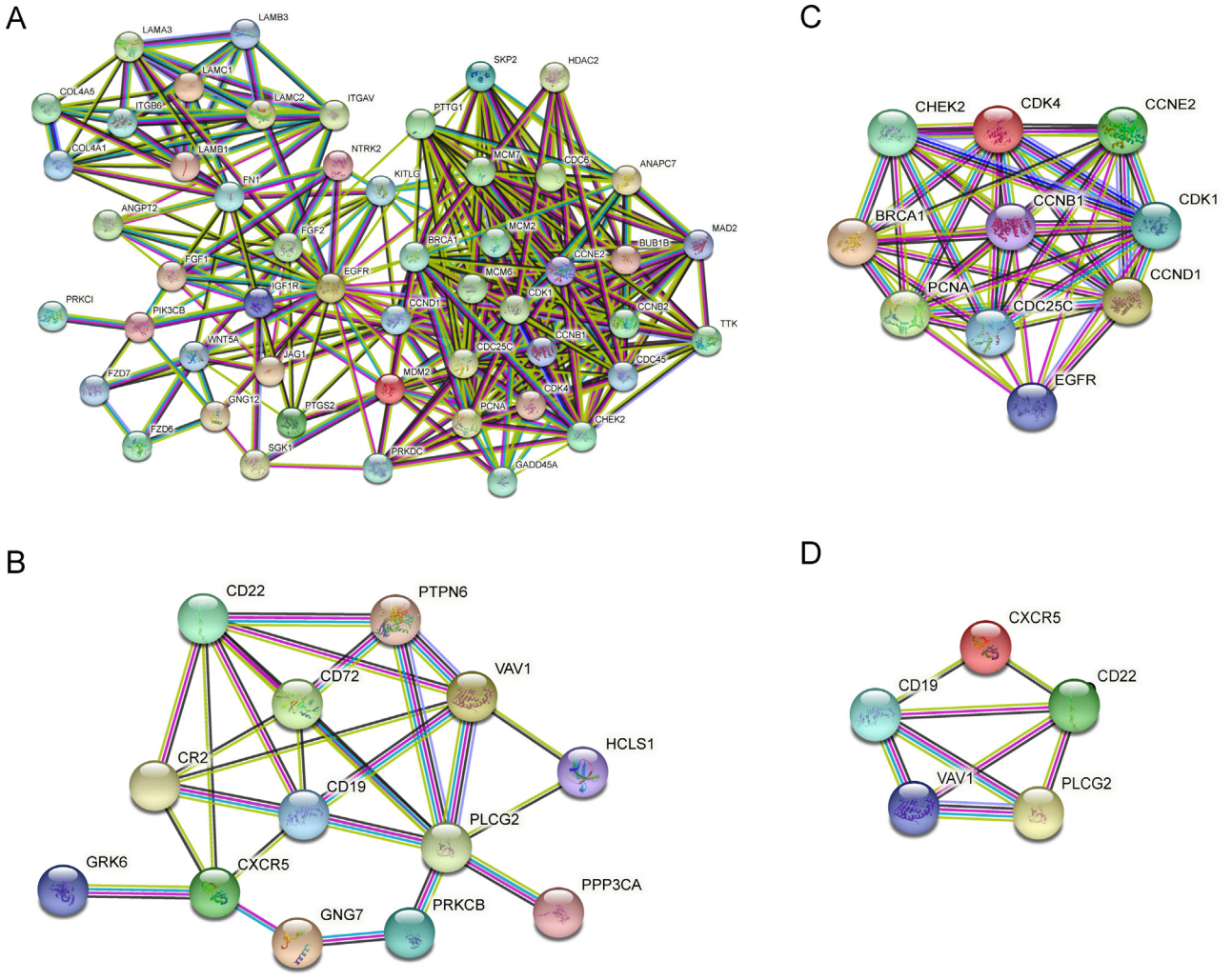

Fig. 10. PPI network presentation. (A-B) PPI network based on the genes of the first three KEGG pathways of gene intersection Ⅰ and gene intersection Ⅱ. (C-D) PPI network based on the hub genes of gene intersection Ⅰ and gene intersection Ⅱ.

25, 24, 24, 22, 22, and 22). The top five hub genes in gene intersection Ⅱ were PLCG2, CD22, VAV1, CD19, and CXCR5 (scores: 8, 7, 6, 6, and 5). Corresponding PPI networks were constructed for these two hub gene groups (Figs. 10C and D).

3.6. Prediction of the upstream transcription factor of ITGAV

The Cistrome DB toolkit predicted 200 TFs, which is shown in Fig. 11A. BRCA1 was not only included in these TFs but also as the hub gene of upregulated DEGs in NPC, which aroused our interest. To further confirm the regulatory effect of BRCA1 on ITGAV, we searched the ChIP-seq data of BRCA1 in Cistrome DB, but there was no relevant sample of NPC tissue or cells. Considering that NPC is an epithelial tumor, we selected epithelial samples for the study, including samples from the cervix, liver, and breast. Near the ITGAV transcription start site (Table 2), these samples all showed specific high signals (Figs. 11B and C). We also obtained the motif of BRCA1 (Figs. 11D and E), which reflected the combination mode of BRCA1. In addition, SMD (95% CI: 0.88–2.59, $p < 0.001$, Fig. 12A) and the AUC value of the SROC curve (95% CI: 0.83–0.89, Fig. 12B) confirmed the high expression of BRCA1 in NPC. The linear correlation analysis of ITGAV and BRCA1 indicated that, except for GSE39826, the other expression matrices demonstrated that the expressions of the two were positively correlated (Figs. 13A-I).

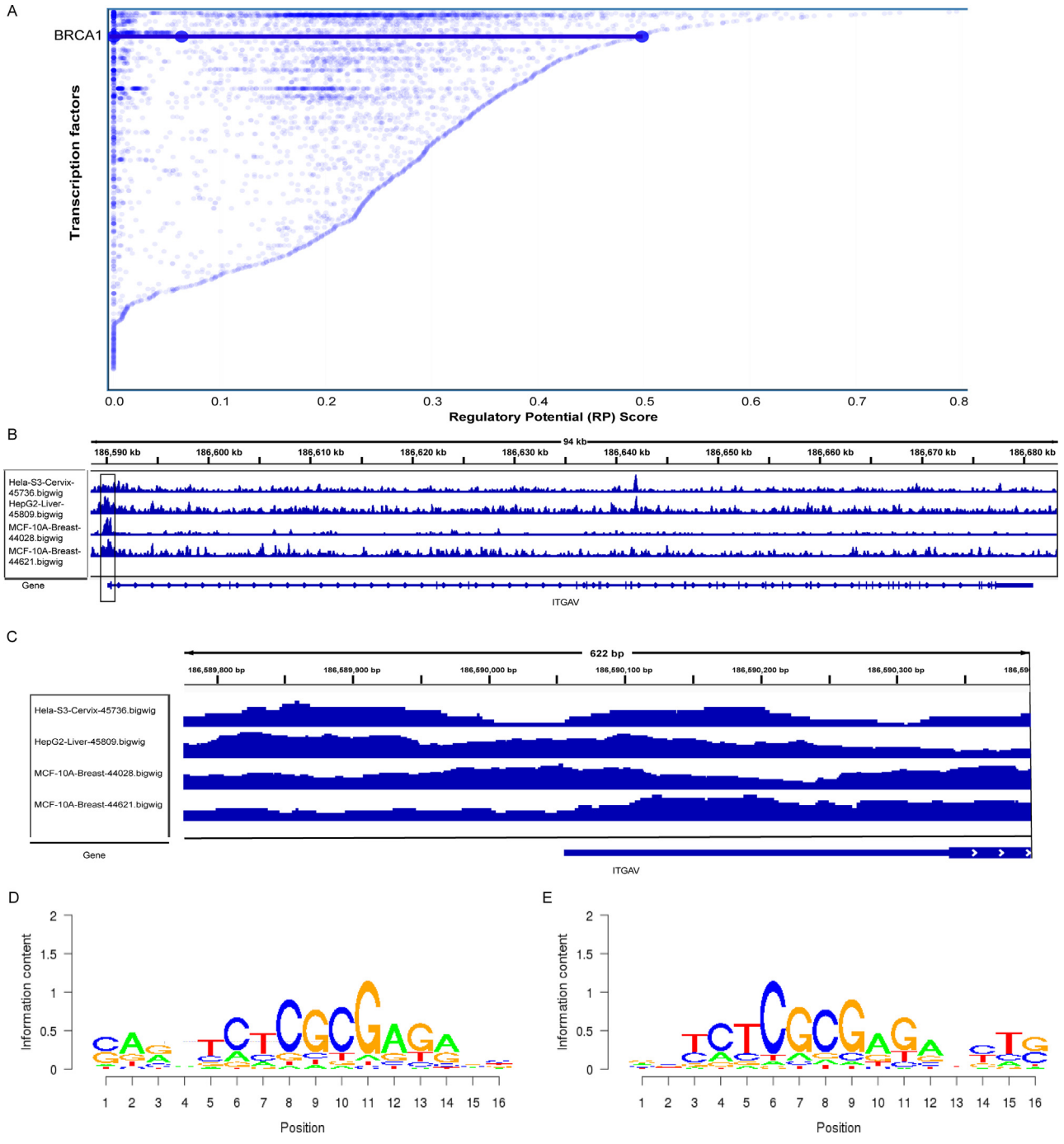

Fig. 11. ChIP-sequencing (ChIP-seq) information for TF BRCA1 from Cistrome Data Browser. (A) TFs with the potential to regulate ITGAV. The Y-axis represents the regulatory potential score calculated via the Cistrome DB Toolkit. The X-axis represents the different TFs. Every dot represents a ChIP-seq sample. (B) ChIP-seq for the full length of ITGAV. (C)Views of specific peaks observed near the promoter region. (D)-(E) Predictive motifs of TF BRCA1.

Table 2
Base sequence information for the peak region of ITGAV in Figure 11C.

TF	Chromosomal region	Peak sequence
BRCA1	chr2:186,589,776–186,590,396	CACGCCTCCTCAGGTGCTC AGCCTGAGGCCTTCGTCCAGGAGCGCTGCCGCTGACCCAGGCTCAGGAGCTGGGGGCCCCT GCACAGACGCCCAGGTCTCGGGAC AGGCGGCGACTGCACTCACGGAAGTACGCTGAGCTCTCCCCTGTAGAAGGGCGCC TCTCCTCCCCCACTT CCTCCTCCAGCTCCACAGCAGCCTCCCGGGCCGGCTCCTCCTCCTTCCAGGTCTCCTCCCAGTGCCGC CGCGG CTCTCAGGCCTGAGGTGCGGCGCTCACCCCGGCAGTCCCCAGCCTCAGACGCTGCGTGGAGCGGCGGAGCCGGA GGGAAGCAAAGGACCGTCTGCGCTGCTGTCCCCGCCCCGCGCGCTCTGCGCCCCTCGTCCCTGGCGGTCGCTCCGAAGCTC AGCCCTCTTGCCTGCCCCGGAGCTGTCCCG GGCTAGCCGAGAAGAGAGCGGCCGGCAAGTTTGGGCGCGCGCAGGCGGC GGGCCGCGGGCACTGGGCGCCTCGCTGGGGCGGGGGGAGGTGGCTACCGCTCCCGGCTTGGCGTCCCGCGCGCACTTCGG CGATGGCTTTTCCGCCGCGGCGACGGCTGCGCCTCGGTCCCCGCGGCCTCCCGCTTCTTCT

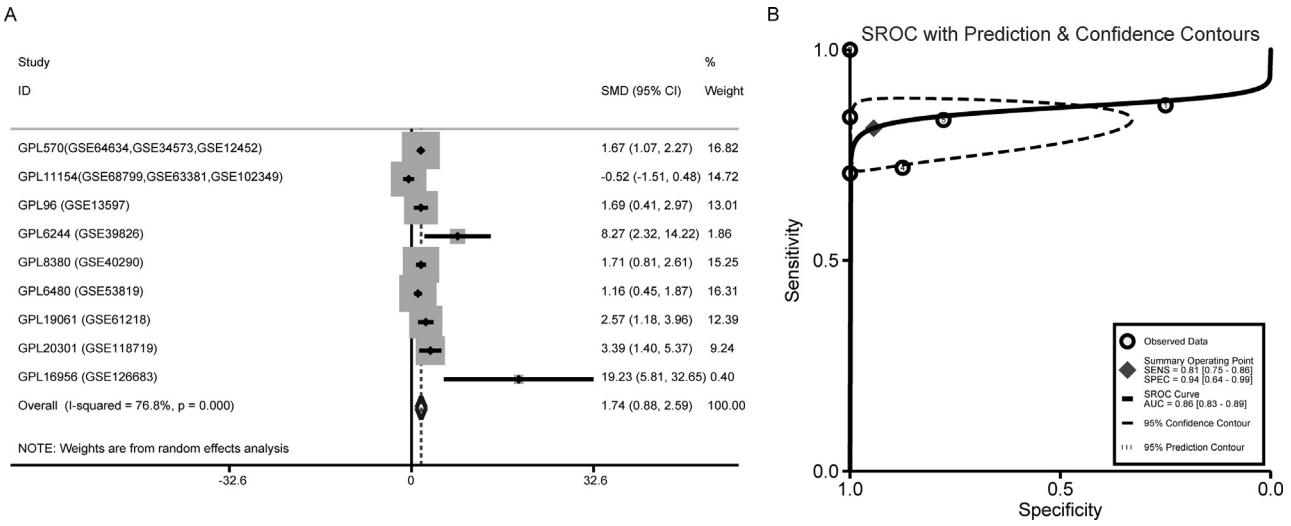

Fig. 12. Analysis of BRCA1 expression level in NPC based on nine datasets. (A) Forest plot for evaluating BRCA1 expression between NPC and control. (B) SROC curve of the distinguishing ability of BRCA1 for NPC from noncancerous samples.

After the conversion calculation of r, the combined r value was 0.39 (95% CI: 0.12–0.61, Fig. 13J), indicating that the co-expression level of ITGAV and BRCA1 was moderate.

4. Discussion

In this study, the results of IHC staining confirmed the overexpression of ITGAV protein in NPC tissues. In addition, the high-throughput data of ITGAV was searched in detail in public gene databases such as TCGA, Oncomine, and GEO. The 13 datasets were analyzed, and it was found that the expression level of ITGAV mRNA in NPC tissue was higher than in noncancerous nasopharyngeal tissue. The results are consistent with previous studies [19,20,21]. However, previous research has been based on single and small sample sizes. In this paper, we selected more samples for IHC detection. The mRNA expression samples from multicenter sources were acquired, and the comprehensive analysis verified the upregulation of ITGAV in NPC.

Acting as a detector for changes in the environment and causing the cell to respond to the external milieu, integrins are bridges that connect the ECM with the cytoskeleton. Moreover, the affinity of integrins to components of the ECM can be changed by intracellular signaling or changes in the cytoskeleton [33]. Regarding the mechanism of ITGAV in NPC, previous research has reported that miR-9-3p inhibits the proliferation, migration, and invasion of NPC cells by downregulating FN1, ITGB1, and ITGAV, which inactivates the EMT process [21]. Moreover, ITGAV was highly expressed in NPC three dimensional spheres and cisplatin-resistant cell lines, and it mediated the generation of drug resistance by inhibiting phosphorylated ERK/caspase-3 [34]. For other cancers, Geertje van der Horst et al. verified that cell migration, stemness, and EMT can be reduced in prostate and bladder cancer by ITGAV knockdown and ITGAV antagonist treatment [35]. Integrins participate in the occurrence and development of cancer by affecting cell proliferation, invasion, and survival in adjacent tissues, as demonstrated by Zhang et al. They also found that integrins can regulate cell survival and apoptosis, thereby promoting the growth and metastasis of tumor tissues [36]. All the above researches confirmed that ITGAV played a role in promoting cancer in NPC and other cancers, which was consistent with this study. In our research, we screened the DEGs in NPC tissues and the co-expressed genes of ITGAV in NPC for intersections, and gene intersection I was obtained, which was analyzed for the enrichment of GO and KEGG pathways. The enrichment analysis of the KEGG pathway based on gene A showed that ITGAV participates in the occurrence and development of NPC mainly by the PI3K-Akt signaling pathway, cell cycle, and human papillomavirus infections. This result provides a new idea for the potential mechanism of ITGAV in NPC.

We created a PPI network with ITGAV and the genes that were positively related to its expression in NPC, and 10 hub genes were screened. Epidermal growth factor receptor (EGFR) and Cyclin B1 (CCNB1) were the top two hub genes. EGFR, also known as HER1 or ErbB1, is a 170 kDa transmembrane receptor composed of three important domains: the extracellular domain, the transmembrane

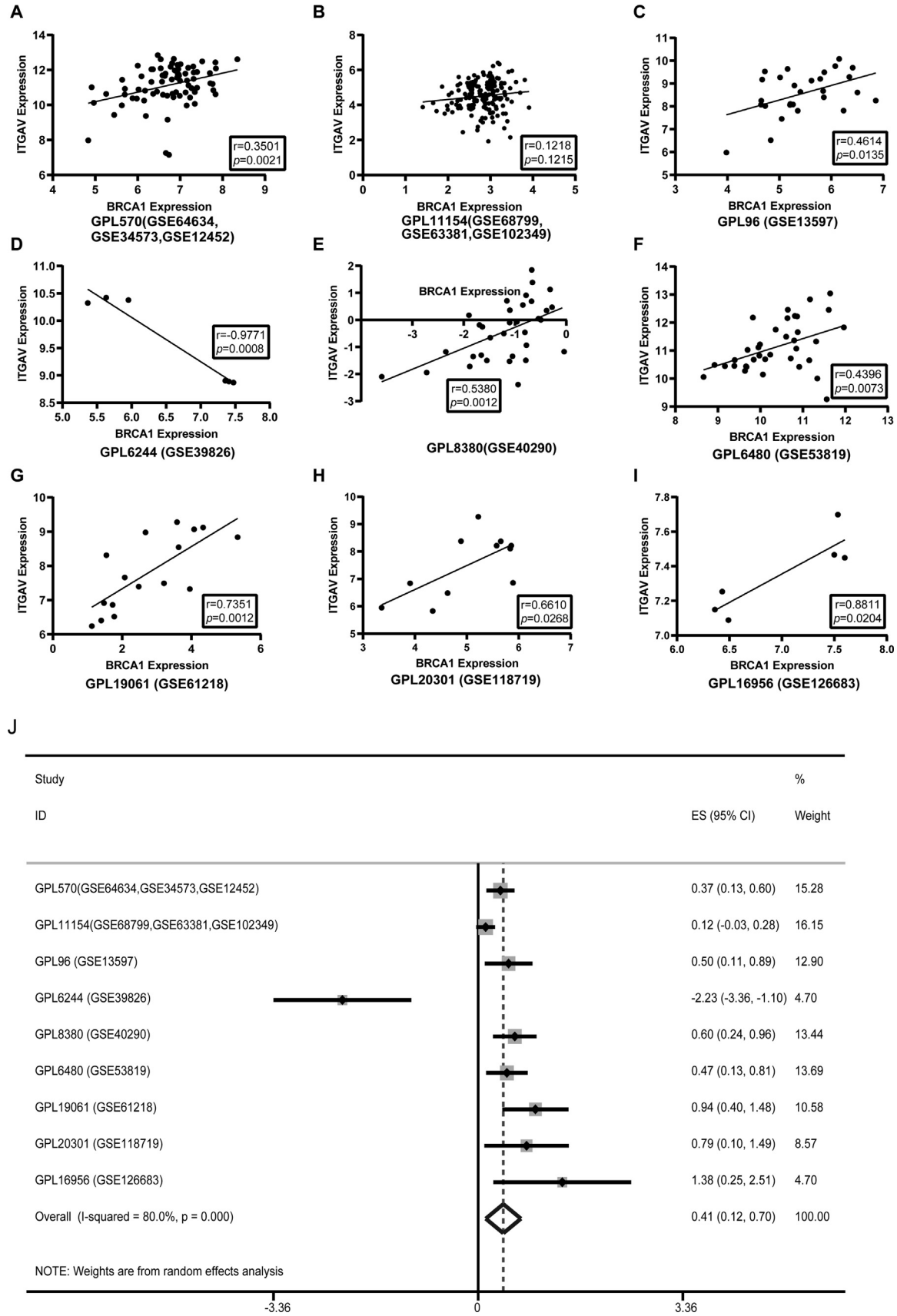

Fig. 13. (A)-(I) The linear graphs of correlation between ITGAV and BRCA1. (J) Forest plot for evaluation of ITGAV and BRCA1 co-expression level.

domain, and the intracellular domain [37]. Receptor-specific ligands can bind to extracellular domains to activate the phosphorylation of receptor tyrosine kinases in the cytoplasmic domain, and then activate downstream pathways, including RAS/RAF/MEK/ERK, JAK/STAT, and PI3K/Akt pathways [38]. Zheng et al. found that SPINK6 enhances epithelial-mesenchymal transition by activating EGFR and downstream AKT pathways, thereby promoting the invasion of NPC [39]. For CCNB1, the lack of expression leads to the disruption of the G2/M cell cycle [40]. In pancreatic cancer, CCNB1 silencing has been shown to inhibit tumor cell proliferation and induce cell senescence and apoptosis through the p53 pathway [41]. These studies inspire us that it can be speculated ITGAV work with these two genes synergistically to promote the canceration and development of NPC.

After predicting the TFs upstream of ITGAV, BRCA1 was selected as one of the TFs for further study. The protein encoded by BRCA1 is involved in many important biological processes, such as DNA damage repair, cell cycle checkpoints, transcription regulation, and ubiquitination modification [42]. Its mutation allows homologous recombination to repair functional defects and leads to the onset of ovarian cancer and breast cancer [43]. Previous studies have reported that BRCA1 mRNA levels are higher in NPC tissues than noncancerous tissues, which is consistent with our research. Furthermore, the inhibition of BRCA1 could make NPC cells more sensitive to chemotherapy [44]. Although research on the BRCA1-targeted regulation of ITGAV is not conclusive, our correlation analysis and publicly available ChIP-seq samples support the potential for a regulatory relationship between the two; more interestingly, in the KEGG analysis, the two were both enriched in the PI3K-Akt signaling pathway. PI3K-Akt signaling is an important intracellular pathway that regulates cell cycle, quiescence, and proliferation. It has been found to be abnormally active in a variety of cancers; moreover, the abnormal activation may lead to the upregulation of BRCA1 [45]. Based on this, we speculate that the aberrant activation of the PI3K-Akt signaling pathway leads to overexpressed BRCA1, which regulates the transcription of ITGAV; this regulatory axis plays a role in promoting cancer in NPC. Based on the above research, we made a hypothesis diagram and presented it in Fig. 14.

Though our research is based on gene expression profile data and clinical samples as much as possible, there are still limitations. The effect of ITGAV on the prognosis of NPC cannot be evaluated due to the lack of data and detailed patient information. In recent years, with the swift development of high-throughput techniques, single-cell sequencing technology has also matured and can be used to further confirm the results of this research. We hope to verify the conclusions of this study by in vitro and in vivo experiments as well as single-cell sequencing technology.

5. Conclusions

We suggest that the upregulation of ITGAV may promote NPC progression through regulation by the TF BRCA1 and interaction with other key genes. ITGAV could be a promising target for NPC therapy. Next, we will design relevant in vitro and in vivo experiments to test our hypothesis.

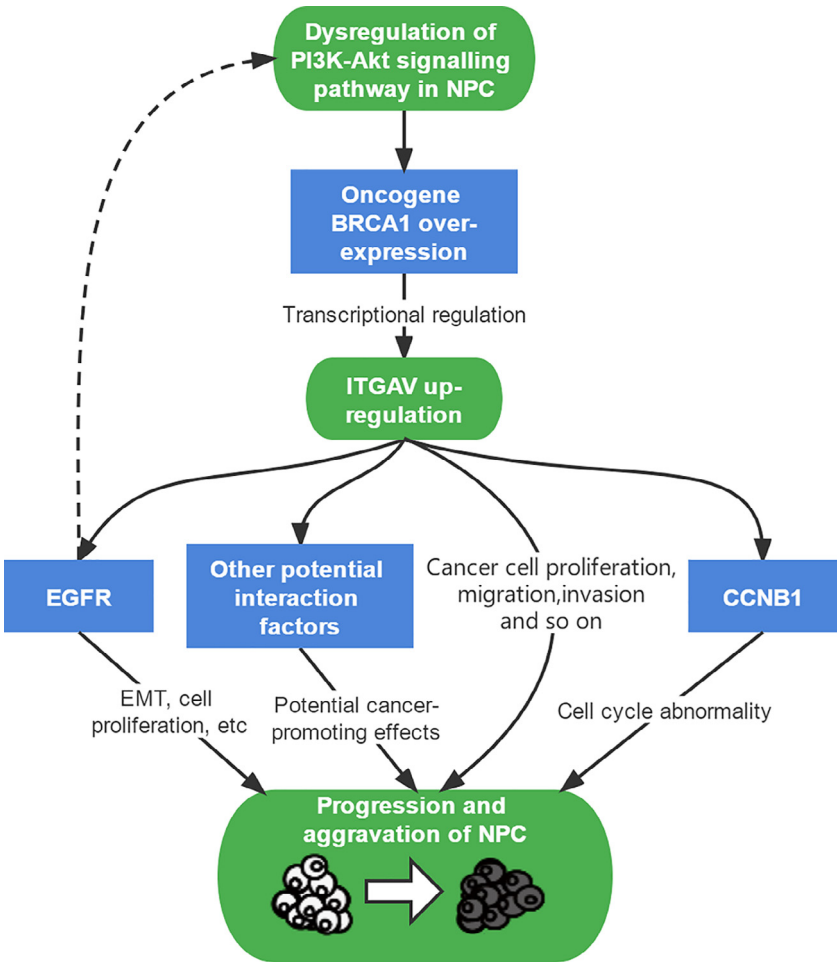

Fig. 14. Hypothesis figure based on the potential role of ITGAV in NPC.

Ethical approval

The present study was approved by the Ethics Committee of The First Affiliated Hospital of Guangxi Medical University, and all patients provided written informed consent.

Author contributors

- Study conception and design: G Chen, Z-G Huang, Y-W Dang
- Data collection: S-W Huang, J-Y Luo
- Analysis and interpretation of results: S-W Huang, J-Y Luo, L-T Qin
- Draft manuscript preparation: S-W Huang, L-T Qin
- Revision of the results and approved the final version of the manuscript: S-N Huang, J He, J-H Zeng, Z-X Wei, W Lu

Financial support

The present study was supported by the Guangxi Medical High-level Key Talents Training "139" Program (2020) and the Guangxi Zhuang Autonomous Region Health Commission Self-financed Scientific Research Project (Z20201236 and Z-A20220491).

Conflict of interest

The authors declare no conflict of interest.

Acknowledgments

The authors would like to thank Guangxi Key Laboratory of Medical Pathology for supporting this study. The authors would also like to thank people who have contributed to the public biology database.

Data availability

The datasets used during the present study are available from the corresponding author upon reasonable request.

References

[1] Liu W, Chen G, Gong X, et al. The diagnostic value of EBV-DNA and EBV-related antibodies detection for nasopharyngeal carcinoma: a meta-analysis. Cancer Cell Int 2021;21(1):164. PMid: 33691680 https://doi.org/10.1186/s12935-021-01862-7.

[2] Xu S, Zhou Z, Peng X, et al. EBV-LMP1 promotes radioresistance by inducing protective autophagy through BNIP3 in nasopharyngeal carcinoma. Cell Death Dis 2021;12(4):344. PMid: 33795637 https://doi.org/10.1038/s41419-021-03639-2.

[3] Zhou X, Lin Y, Chen Y, et al. Epstein-Barr virus (EBV) encoded microRNA BART8-3p drives radioresistance-associated metastasis in nasopharyngeal carcinoma. J Cell Physiol 2021;236(9):6457–71. PMid: 33694159 https://doi.org/10.1002/jcp.30320.

[4] Feng G, Xu Y, Ma N, et al. Influence of Epstein-Barr virus and human papillomavirus infection on macrophage migration inhibitory factor and macrophage polarization in nasopharyngeal carcinoma. BMC Cancer 2021;21(1):929. PMid: 34407796 https://doi.org/10.1186/s12885-021-08675-x.

[5] Chen WJ, Xu WN, Wang HY, et al. Plasma Epstein-Barr virus DNA and risk of nasopharyngeal carcinoma in a prospective seropositive population. BMC Cancer 2021;21(1):651. PMid: 34074258 https://doi.org/10.1186/s12885-021-08408-0.

[6] Lu W, Luo JY, Wu MH, et al. Expression of vimentin in nasopharyngeal carcinoma and its possible molecular mechanism: A study based on immunohistochemistry and bioinformatics analysis. Pathol Res Pract 2019;215(5):1020–32. PMid: 30833029 https://doi.org/10.1016/j.prp.2019.02.010.

[7] Wu LZ, Huang ML, Qi CL, et al. Overexpression of Notch2 enhances radiosensitivity via inhibition of the AKT/mTOR signaling pathway in nasopharyngeal carcinoma. Bioengineered 2021;12(1):3398–409. PMid: 34224316 https://doi.org/10.1080/21655979.2021.1949236.

[8] Lai C, Zhang C, Lv H, et al. A novel prognostic model predicts overall survival in patients with nasopharyngeal carcinoma based on clinical features and blood biomarkers. Cancer Med 2021;10(11):3511–23. PMid: 33973727 https://doi.org/10.1002/cam4.3839.

[9] Kyrodimos E, Chrysovergis A, Mastronikolis N, et al. Targeting EGFR in nasopharyngeal carcinoma. J Buon 2021;26(3):759–61. PMid: 34268932.

[10] Liang T, Liu W, Xie J, et al. Serum EA-IgA and D-dimer, but not VCA-IgA, are associated with prognosis in patients with nasopharyngeal carcinoma: a meta-analysis. Cancer Cell Int 2021;21(1):329. PMid: 34193149 https://doi.org/10.1186/s12935-021-02035-2.

[11] Yang JH, Sun XS, Xiao BB, et al. Subdivision of de-novo metastatic nasopharyngeal carcinoma based on tumor burden and pretreatment EBV DNA for therapeutic guidance of locoregional radiotherapy. BMC Cancer 2021;21(1):534. PMid: 33975558 https://doi.org/10.1186/s12885-021-08246-0.

[12] Hamidi H, Ivaska J. Every step of the way: integrins in cancer progression and metastasis. Nat Rev Cancer 2018;18(9):533–48. PMid: 30002479 https://doi.org/10.1038/s41568-018-0038-z.

[13] Demircioglu F, Hodivala-Dilke K. αvβ3 Integrin and tumour blood vessels-learning from the past to shape the future. Curr Opin Cell Biol 2016;42:121–7. PMid: 27474973 https://doi.org/10.1016/j.ceb.2016.07.008.

[14] Alday-Parejo B, Stupp R, Ruegg C. Are integrins still practicable targets for anti-cancer therapy? Cancers (Basel) 2019;11(7):978. PMid: 31336983 https://doi.org/10.3390/cancers11070978.

[15] Wang H, Chen H, Jiang Z, et al. Integrin subunit alpha v promotes growth, migration, and invasion of gastric cancer cells. Pathol Res Pract 2019;215(9):. PMid: 31320250 https://doi.org/10.1016/j.prp.2019.152531152531.

[16] Weiler SME, Lutz T, Bissinger M, et al. TAZ target gene ITGAV regulates invasion and feeds back positively on YAP and TAZ in liver cancer cells. Cancer Lett 2020;473:164–75. PMid: 31904487 https://doi.org/10.1016/j.canlet.2019.12.044.

[17] Cheuk IW, Siu MT, Ho JC, et al. ITGAV targeting as a therapeutic approach for treatment of metastatic breast cancer. Am J Cancer Res 2020;10(1):211–23. PMid: 32064162.

[18] Pei Y, Zhang Y, Zheng K, et al. *Ilex hainanensis Merr* targets ITGAV to suppress the proliferation and metastasis of osteosarcoma cells. Onco Targets Ther 2019;12:4499–507. PMid: 31239718 https://doi.org/10.2147/OTT.S205688.

[19] Xuan SH, Zhou YG, Pan JQ, et al. Overexpression of integrin αv in the human nasopharyngeal carcinoma associated with metastasis and progression. Cancer Biomark 2013;13(5):323–8. PMid: 24440971 https://doi.org/10.3233/CBM-130361.

[20] Ou J, Luan W, Deng J, et al. αV integrin induces multicellular radioresistance in human nasopharyngeal carcinoma via activating SAPK/JNK pathway. PLoS ONE 2012;7(6):e38737. PMid: 22719931 https://doi.org/10.1371/journal.pone.0038737.

[21] Ding Y, Pan Y, Liu S, et al. Elevation of MiR-9-3p suppresses the epithelial-mesenchymal transition of nasopharyngeal carcinoma cells via down-regulating FN1, ITGB1 and ITGAV. Cancer Biol Ther 2017;18(6):414–24. PMid: 28613134 https://doi.org/10.1080/15384047.2017.1323585.

[22] Zhang Y, Li ZY, Hou XX, et al. Clinical significance and effect of AEG-1 on the proliferation, invasion, and migration of NSCLC: a study based on immunohistochemistry, TCGA, bioinformatics, *in vitro* and *in vivo* verification. Oncotarget 2017;8(10):16531–52. PMid: 28152520 https://doi.org/10.18632/oncotarget.14972.

[23] Zheng HP, Huang ZG, He RQ, et al. Integrated assessment of CDK1 upregulation in thyroid cancer. Am J Transl Res 2019;11(12):7233–54. PMid: 31934275.

[24] Gao L, Pang YY, Guo XY, et al. Polo like kinase 1 expression in cervical cancer tissues generated from multiple detection methods. PeerJ 2020;8:e10458. PMid: 33354424 https://doi.org/10.7717/peerj.10458.

[25] Li R, Chen G, Dang Y, et al. Upregulation of ATIC in multiple myeloma tissues based on tissue microarray and gene microarrays. Int J Lab Hematol 2021;43(3):409–17. PMid: 33226193 https://doi.org/10.1111/ijlh.13397.

[26] Qiu LL, Zhang XG, Chen G, et al. Clinical significance of the interleukin 24 mRNA level in head and neck squamous cell carcinoma and its subgroups: an in silico investigation. J Oncol 2020;2020:7042025. PMid: 33014054 https://doi.org/10.1155/2020/7042025.

[27] Sun Y, Chen G, He J, et al. Clinical significance and potential molecular mechanism of miRNA-222-3p in metastatic prostate cancer. Bioengineered 2021;12(1):325–40. PMid: 33356818 https://doi.org/10.1080/21655979.2020.1867405.

[28] Gan XN, Gan TQ, He RQ, et al. Clinical significance of high expression of miR-452-5p in lung squamous cell carcinoma. Oncol Lett 2018;15(5):6418–30. PMid: 29616113 https://doi.org/10.3892/ol.2018.8088.

[29] Li J, Rong MH, Dang YW, et al. Differentially expressed gene profile and relevant pathways of the traditional Chinese medicine cinobufotalin on MCF7 breast cancer cells. Mol Med Rep 2019;19(5):4256–70. PMid: 30896874 https://doi.org/10.3892/mmr.2019.10062.

[30] Huang ZG, Sun Y, Chen G, et al. MiRNA-145-5p expression and prospective molecular mechanisms in the metastasis of prostate cancer. IET Syst Biol 2021;15(1):1–13. PMid: 33527765 https://doi.org/10.1049/syb2.12011.

[31] Zheng R, Wan C, Mei S, et al. Cistrome Data Browser: expanded datasets and new tools for gene regulatory analysis. Nucleic Acids Res 2019;47(D1):D729–35. PMid: 30462313 https://doi.org/10.1093/nar/gky1094.

[32] Wang S, Sun H, Ma J, et al. Target analysis by integration of transcriptome and ChIP-seq data with BETA. Nat Protoc 2013;8(12):2502–15. PMid: 24263090 https://doi.org/10.1038/nprot.2013.150.

[33] Ginsberg MH. Integrin activation. BMB Rep 2014;47(12):655–9. PMid: 25388208 https://doi.org/10.5483/bmbrep.2014.47.12.241.

[34] Ngaokrajang U, Janvilisri T, Sae-Ueng U, et al. Integrin α5 mediates intrinsic cisplatin resistance in three-dimensional nasopharyngeal carcinoma spheroids via the inhibition of phosphorylated ERK /caspase-3 induced apoptosis. Exp Cell Res 2021;406(2):. PMid: 34358523 https://doi.org/10.1016/j.yexcr.2021.112765112765.
[35] van der Horst G, Bos L, van der Mark M, et al. Targeting of α-v integrins reduces malignancy of bladder carcinoma. PLoS ONE 2014;9(9):e108464. PMid: 25247809 https://doi.org/10.1371/journal.pone.0108464.
[36] Zhang CH, Xu GL, Jia WD, et al. Prognostic significance of osteopontin in hepatocellular carcinoma: a meta-analysis. Int J Cancer 2012;130(11):2685–92. PMid: 21780114 https://doi.org/10.1002/ijc.26301.
[37] Wang Z. ErbB Receptors and Cancer. Methods Mol Biol 2017;1652:3–35. PMid: 28791631 https://doi.org/10.1007/978-1-4939-7219-7_1.
[38] Xu MJ, Johnson DE, Grandis JR. EGFR-targeted therapies in the post-genomic era. Cancer Metastasis Rev 2017;36(3):463–73. PMid: 28866730 https://doi.org/10.1007/s10555-017-9687-8.
[39] Zheng LS, Yang JP, Cao Y, et al. SPINK6 promotes metastasis of nasopharyngeal carcinoma via binding and activation of epithelial growth factor receptor. Cancer Res 2017;77(2):579–89. PMid: 27671677 https://doi.org/10.1158/0008-5472.CAN-16-1281.
[40] Wang J, Chang L, Lai X, et al. Tetrandrine enhances radiosensitivity through the CDC25C/CDK1/cyclin B1 pathway in nasopharyngeal carcinoma cells. Cell Cycle 2018;17(6):671–80. PMid: 29285984 https://doi.org/10.1080/15384101.2017.1415679.
[41] Zhang H, Zhang X, Li X, et al. Effect of CCNB1 silencing on cell cycle, senescence, and apoptosis through the p53 signaling pathway in pancreatic cancer. J Cell Physiol 2018;234(1):619–31. PMid: 30069972 https://doi.org/10.1002/jcp.26816.
[42] Liu J, Adhav R, Miao K, et al. Characterization of *BRCA1*-deficient premalignant tissues and cancers identifies *Plekha5* as a tumor metastasis suppressor. Nat Commun 2020;11(1):4875. PMid: 32978388 https://doi.org/10.1038/s41467-020-18637-9.
[43] Yoshino Y, Fang Z, Qi H, et al. Dysregulation of the centrosome induced by BRCA1 deficiency contributes to tissue-specific carcinogenesis. Cancer Sci 2021;112(5):1679–87. PMid: 33606355 https://doi.org/10.1111/cas.14859.
[44] Lung RW, Tong JH, Ip LM, et al. EBV-encoded miRNAs can sensitize nasopharyngeal carcinoma to chemotherapeutic drugs by targeting BRCA1. J Cell Mol Med 2020;24(22):13523–35. PMid: 33074587 https://doi.org/10.1111/jcmm.16007.
[45] Zhu Y, Liu Y, Zhang C, et al. Tamoxifen-resistant breast cancer cells are resistant to DNA-damaging chemotherapy because of upregulated BARD1 and BRCA1. Nat Commun 2018;9(1):1595. PMid: 29686231 https://doi.org/10.1038/s41467-018-03951-0.